Amino acid modified copper electrodes for the enhanced selective electroreduction of carbon dioxide towards hydrocarbons

Xie, Ming Shi; Xia, Bao Yu; Li, Yawei; Yan, Ya; Yang, Yanhui; Sun, Qiang; Chan, Siew Hwa; Fisher, Adrian; Wang, Xin

2016

Xie, M. S., Xia, B. Y., Li, Y., Yan, Y., Yang, Y., Sun, Q., et al. (2016). Amino acid modified copper electrodes for the enhanced selective electroreduction of carbon dioxide towards hydrocarbons. Energy & Environmental Science, 9(5), 1687-1695.

https://hdl.handle.net/10356/84389

https://doi.org/10.1039/C5EE03694A

Energy & Environmental Science

ARTICLE

Amino Acid Modified Copper Electrodes for the Enhanced Selective Electroreduction of Carbon Dioxide towards Hydrocarbons

Received 00th January 20xx,
Accepted 00th January 20xx

DOI: 10.1039/x0xx00000x

www.rsc.org/

Ming Shi Xie,[a] Bao Yu Xia,[a] Yawei Li,[b] Ya Yan,[a] Yanhui Yang,[a] Qiang Sun,[b] Siew Hwa Chan,[c] Adrian Fisher,[d] and Xin Wang*[a]

Electroreduction of carbon dioxide to hydrocarbons has been proposed as a promising way to utilize CO_2 and maintain carbon balance in the environment. Copper (Cu) is an effective electrocatalyst for such purpose. However, the overall selectivity towards hydrocarbons on Cu-based electrodes is still very limited. In this work, we develop a general amino acid modification approach on Cu electrodes for selective electroreduction of CO_2 towards hydrocarbons. Remarkable enhancement in hydrocarbon generation is achieved on these modified copper electrodes, regardless of the morphology of the Cu electrodes. A density functional theory calculation reveals that the key intermediate CHO* is stabilized by interacting with $–NH_3^+$ of the adsorbed zwitterionic glycine. Our results suggest that amino acids and their derivatives are promising modifiers in improving the selectivity of hydrocarbons in CO_2 electroreduction.

using

1. Introduction

Carbon dioxide (CO_2) is the primary greenhouse gas emitted through human activities. Since the industrial revolution, fossil fuel combustion has rapidly increased its concentration in the atmosphere, leading to drastic environmental concern.[1] CO_2 conversion has been proposed as a potential way to maintain balance in the carbon cycle and develop a sustainable society, and many kinds of technologies like photocatalytic reduction and Fischer-Tropsch synthesis have been already applied in this area.[2-7] In line with this, electrochemical reduction of CO_2 to hydrocarbons renewable energy is attractive due to its high conversion efficiency and desirability of the hydrocarbon-based products that can be obtained.[8-12] Many electrocatalysts including metal and molecule pyridine catalysts have been investigated for CO_2 reduction in the past decades.[13-25] Of all the metals examined hitherto, only copper (Cu) has shown a unique ability to produce hydrocarbons with reasonable Faradaic efficiency (FE).[26, 27] Achieving high efficiency in the Cu-catalyzed CO_2 reduction process requires Cu electrodes with sufficient active sites.[28] Various nanostructured Cu electrodes have thus been reported to enhance the activity and selectivity.[29-33] Nevertheless, the overall selectivity towards hydrocarbons is still very limited.[34] Particularly, the final hydrocarbon mixtures obtained are mostly composed of methane (CH_4) and ethylene (C_2H_4).[35-38] Typically, only very small amounts of ethane (C_2H_6) are produced, and high carbon products like propene (C_3H_6) are even rarer.[39]

Theoretical calculations reveal that effective catalysts must be capable of efficiently catalyzing the protonation of adsorbed CO to adsorbed CHO or COH and exhibit simultaneous poor activity for the competitive hydrogen evolution reaction.[40, 41] It is further proposed that the presence of certain ligands on the catalyst surface would stabilize such adsorbed intermediates (CHO or COH)

[a] School of Chemical and Biomedical Engineering, Nanyang Technological University, 62 Nanyang Drive, Singapore 637459, Singapore
E-mail: WangXin@ntu.edu.sgs
[b] Singapore-Peking University Research Centre, Campus for Research Excellence & Technological Enterprise (CREATE), Singapore 138602, Singapore Department of Materials Science and Engineering, Peking University, Beijing 100871, China.
[c] School of Mechanical & Aerospace Engineering, Nanyang Technological University, 50 Nanyang Avenue, Singapore 639798, Singapore
[d] Department of Chemical Engineering and Biotechnology, University of Cambridge, New Museums Site, Pembroke Street, Cambridge, CB2 3RA, UK

† Electronic Supplementary Information (ESI) available: Detailed experiments, FESEM images, EDX results, contact angel measurements, EIS results, XPS spectrums, complete form of faradaic efficiencies, electrochemical surface area measurement, GC diagrams and other electrochemical results. See DOI: 10.1039/x0xx00000x

over CO, the selectivity to hydrocarbons could then be improved.[42] Unfortunately, no experimental evidence has ever been reported to support such theoretical prediction. Along this direction, we describe our recent efforts in developing amino acid modified Cu electrodes for enhanced hydrocarbon production. To demonstrate the validity of this novel modification approach and to rule out any possible Cu morphology effect, we examined three different types of Cu electrodes, namely, Cu nanowire (NW) film, smooth Cu foil, and annealed Cu electrode.[43] The choice of amino acid to modify Cu surface is based on the fact that amino acids and their derivatives have been used to modify metal catalysts for hydrogenating carbonyl compounds, and the enhanced interaction between certain functional groups of amino acids and intermediate CHO.[44, 45]

We demonstrate herein that the remarkably enhanced Faradaic efficiency (FE) of total hydrocarbons, including C2 hydrocarbons (C_2H_4 and C_2H_6) and a small amount of C3 hydrocarbon (C_3H_6), increases by up to 100% for glycine modified Cu NW film. Similar trends are also observed on the other two types of Cu electrodes, where the FEs of total hydrocarbons on the modified Cu foil and annealed Cu electrodes have also more than doubled. To the best of our knowledge, this is the first report to realize the enhanced selectivity of Cu electrodes in producing hydrocarbons via the surface modification method. The mechanism of such enhancement is further illustrated by theoretical calculation. Excellent adsorption stability of amino acids on Cu surface during the electrochemical process is also demonstrated.

2. Experimental Section

2.1 Preparation of electrodes. Cu foils (20 mm×20 mm) were first electropolished in 85 wt. % phosphoric acid at 0.5 V vs. Ag/AgCl for 500 s. Polished Cu foils were washed with deionized water, and then immediately immersed into a chemical bath, which is prepared with sodium hydroxide (2.0 g), potassium persulfate (0.81 g) and deionized water (20 mL). After 4 h, a film of copper hydroxide ($Cu(OH)_2$ NW film) were generated, and then it was washed with deionized water. $Cu(OH)_2$ NW film was electrochemical reduced in 0.1 M $KHCO_3$ solution at -2.0 V for 500 s in to obtain Cu nanowire file electrodes (Cu NW film). Annealed-reduced Cu electrodes were prepared by annealing at 500 ^{o}C under the air for 12 h in muffle furnace, and then *in-situ* electrochemical reducing at -2.0 V for 500 s in our cell according to the previous report.[43] In this process, the Cu electrodes were first oxidized to Cu_2O film and then reduced to Cu electrode. For the modification part, all kinds of amino acids (glycine, DL-alanine, DL-leucine, DL-tryptophan, DL-tyrosine and DL-arginine) were dissolved in deionized water, and 1-dodecyl mercaptan as well as stearic acid was dissolved in ethanol to prepare solution with certain concentrates: 0.1 mM, 0.5 mM, 1.0 mM, 2.5 mM and 10 mM. Electrodes modified by amino acids, mercaptan or stearic acid were prepared by transferring 20 µL solution on each side of one Cu NW film electrode (40 µL in total), then kept for 15 mins and dried under nitrogen flow. Cu foil electrodes were modified through immersing one electropolished Cu foil into ~10 mL water solution which contained 5×10^{-8} mmol glycine. The solution was bubbled with nitrogen for 0.5 h in advance. Diazo salts of anthraquinone and o-nitrobenzene were prepared through typical diazotization of corresponding amine, 1-aminoanthraquinone and o-nitroaniline. Amine was first dissolved in 50 mL HCl (37%), and then 1 m mol $NaNO_2$ is dissolved in 50 mL of deionized water. $NaNO_2$ solution was added into amine solution slowly under ice bath. After stirring for 10 h, 2 µL of reaction mixture containing diazo salt was added into 30 mL acetonitrile solution with 0.1 M NBu_4BF_4. Cu NW film electrodes were electroplated in diazo salt solution at -0.3 V vs. Ag/AgCl for 300 s and then washed with acetonitrile for 3 times to obtain diazo salt modified electrodes.

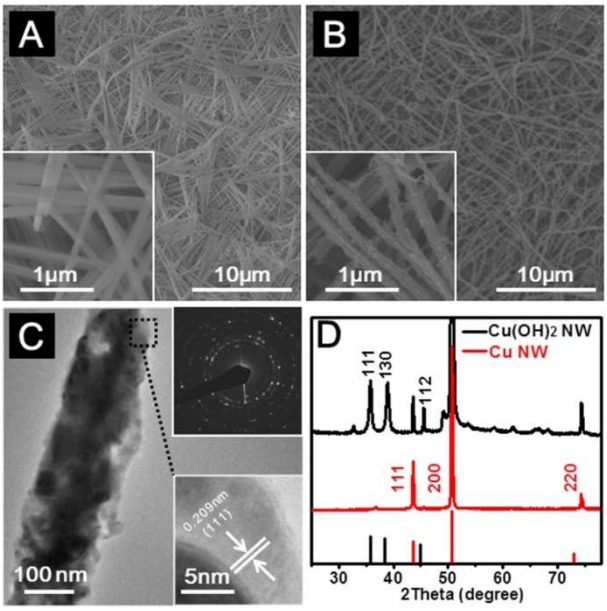

Figure 1. FESEM of $Cu(OH)_2$ NW film (A) and Cu NW film (B). TEM of an individual Cu nanowire (C), the insets in (C) show the selected area electron diffraction (SAED) and HRTEM of Cu NW. XRD patterns (D) of $Cu(OH)_2$ NW film and Cu NW film.

2.2 Electrochemical experiments. An original design H-type cell separated by NAFION N117 ion exchange membrane, and an Autolab potentiostat/galvanostat (Model PGSTAT-72637) workstation at ambient temperature were used for all electrochemical experiments and tests. 0.1 M potassium bicarbonate was prepared with deionized water and used as electrolyte. A Platinum electrode was used as counter electrode in the anode cell, while various Cu electrodes and Ag/AgCl (saturated AgCl) electrodes were used as working electrodes and reference electrodes in the cathode cell. Before electroreduction of CO_2, CO_2 gas was passed through the electrolyte for at least 1 hour to ensure saturated. Headspace of cathode cell was directly linked to a gas chromatograph (Agilent 6890N-G1540N) equipped with a thermal conductivity detector, Porapak Q column and Molecular Sieve 5A column to analyze gas products.

Electrochemical impedance spectroscopy (EIS) was used to prove the stability of absorbed amino acids during electrolysis. A Cu NW film electrode, a modified Cu NW film electrode modified with glycine by immersing into 1.0 mM glycine for 15 mins, and a modified Cu NW film electrode prepared as above which had already worked for 6 h at -1.9 V vs. Ag/AgCl in 0.1 M $KHCO_3$ solution were tested. Each sample was firstly immersed into 0.5 M NaCl solution for 30 mins, and then impedance measurements were

carried out for each sample at open circuit potential, in a frequency range of 10 kHz – 20 mHz and amplitude of 5 mV peak-to-peak using as signals.

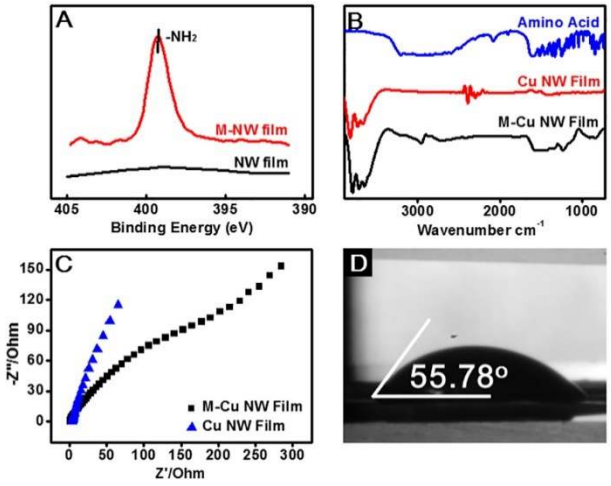

Figure 2. (A) N1s scan XPS patterns of Cu NW film and modified Cu NW film (pre-electrolysis). (B) Fourier transform infrared spectroscopy (FT-IR) of amino acid (tyrosine) KBr pellet, attenuated total reflection infrared spectroscopy (ATR) of Cu NW film and ATR of amino acid modified Cu NW film. (C) Electrochemical impedance spectroscopy (EIS) results of Cu NW film and modified Cu NW film at open circuit potential. (D) Contact angles of Cu NW film modified by 20μL 1mM glycine.

2.3 Characterization. Powder X-ray diffraction (XRD) patterns were obtained by using a Bruker diffractometer with Cu Kα radiation (D8 Advance X-ray diffractometer, Cu Kα, λ = 1.5406 Å, 40 kV, and 40 mA) to get the crystallographic information of the materials. Field-emission scanning electron microscopy (FESEM; JEOL, JSM-6701F, 5 kV) equipped with energy dispersive X-ray spectroscopy (EDX) was used to observe the morphology and elemental composition of the materials. The morphology and microstructure of the products were further studied by transmission electron microscopy (TEM; JEOL, JEM-2010, 200 kV). Fourier transform infrared spectroscopy (FT-IR, Perkin Elmer, equipped with an ATR detector) and attenuated total reflection infrared spectroscopy (ATR) were used to obtain the transmission and reflection infrared spectrum of samples. Tyrosine was used instead of glycine, for its signals of phenyl is obvious. Contact angle analyzer (FTA200 Dynamic Contact Angle Analyzer equipped with an APPRO camera) was used to measure the contact angle of samples. X-ray photoelectron spectroscopy (XPS; VG ESCALAB MKII instrument) with an Mg Kα X-ray source was used for analyzing the surface properties of the samples.

2.4 Theoretical calculations. Density functional theory (DFT) calculations were performed using the Vienna ab initio simulation package (VASP)[46] with the Perdew-Burke-Ernzerhof (PBE) exchange-correlation functional.[47] Ionic cores were treated using the projector-augmented wave (PAW) method.[48] The Cu(110) surfaces were chosen to model the experimental systems due to their enhanced activities towards CO_2 and CO electroreduction.[49] We modeled the surfaces with a 3×3 supercell and 4 metal layers. During the structure optimization, two layers of the adsorbate and the topmost were allowed to relax while the bottommost two layers were kept fixed. Wave functions of valence electrons were expanded using plane wave basis sets with a kinetic energy cutoff of 400 eV. The Brillouin

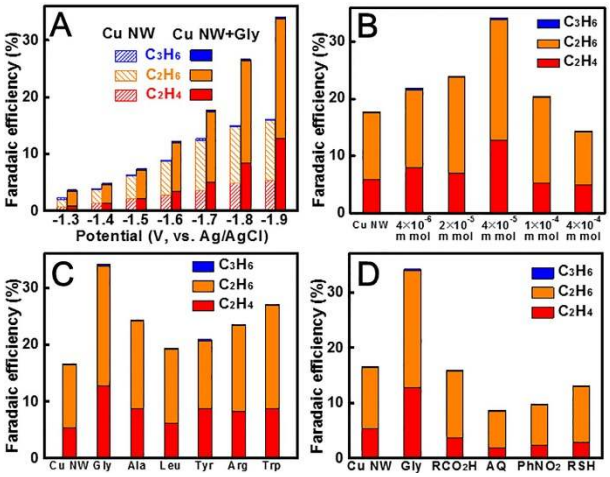

Figure 3. Electrochemical CO_2 reduction on Cu NW film electrodes. (A) On full potential range from -1.3 V to -1.9 V. (B) With different concentrations of glycine at -1.9 V. (C) With different kinds of amino acids at -1. 9 V. (D) With different kinds of modifiers at -1.9 V.

zones were sampled using Monkhorst-Pack scheme with 5×7×1 grids.[50] The Fermi level of surfaces was smeared by the Methfessel-Paxton approach with a Gaussian width of 0.2 eV. To address the solvation effect in the electrochemical environment, we obtained the free energy changes in the proton-coupled electron transfer (PCET) steps using the well-documented computational hydrogen electrode (CHE) model.[51] Solvation corrections of -0.25 eV for ROH and -0.10 eV for carbonyls were applied arising from our test molecular dynamics (MD) simulations including two water layers. The zero-point energies (ZPE) and vibrational contributions to the entropy for different adsorbates were considered within the harmonic oscillator approximation.

3 Results and Discussion

The Cu NW film is obtained by electrochemically reduction of $Cu(OH)_2$ NW film on Cu foil in $KHCO_3$ solution. The thickness of the film is estimated to be 0.8 μm (Experimental details please see Electronic Supplementary Information, ESI). Figure 1A shows field-emission scanning electron microscopy (FESEM) image of $Cu(OH)_2$ NW film, the entire Cu foil surface is uniformly coated with $Cu(OH)_2$ NW. FESEM image obtained at a higher magnification (inset of Figure 1A) further reveals that nanowires formed are 100-200 nm in diameter and tens of micrometers in length. After electrochemical reduction, the Cu NWs retain their one-dimensional morphology, however, the straight nanowires become sinuous while the surfaces of nanowires are roughened (Figure 1B). The structure of the Cu NWs is further investigated by transmission electron microscope (TEM). Figure 1C shows the porous surface of an individual Cu NW. The porous structure and the rough surface should result from dehydration of $Cu(OH)_2$ NW during the reduction process. Selected-area electron diffraction (SAED) pattern (inset of Figure 1C) of single

Cu NW shows concentric rings, composed of bright discrete diffraction spots, indicative of high crystallinity. High resolution (HR) TEM image reveals Cu NW has a lattice fringe with interplane spacing of 0.209 nm, corresponding to the (111) plane of Cu. The Cu NW film is also monitored with X-ray diffraction (XRD) and energy dispersive

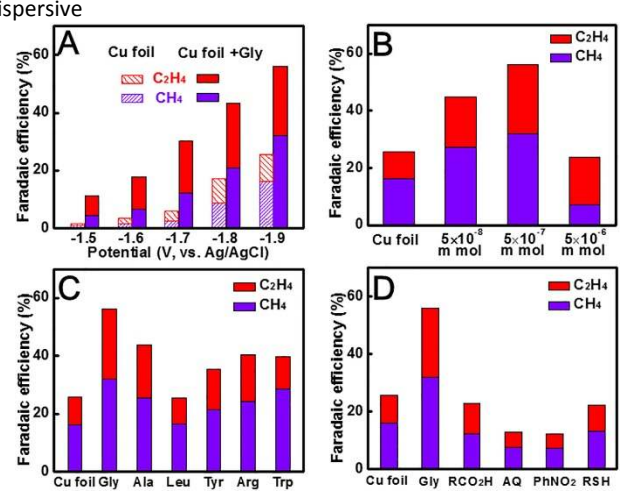

Figure 4. Electrochemical CO_2 reduction on Cu foil electrodes. (A) On full potential range from -1.5 V to -1.9 V. (B) With different amount of glycine at -1.9 V. (C) With different kinds of amino acids at -1.9 V. (D) With different kinds of modifiers at -1.9 V.

X-ray (EDX) techniques (Figure 1D and Figure S1, see the ESI). After treatment of Cu foil in NaOH and $K_2S_2O_8$ chemical bath, diffraction peaks in XRD pattern and EDX analysis indicate the formation of $Cu(OH)_2$ phase. However, peaks ascribed to metallic Cu(0) are still present, indicating that the $Cu(OH)_2$ NW film is not dense enough to completely cover the entire surface of Cu foil base without leaving microvoids. Only Cu(0) peaks are observed after the electroreduction, demonstrating that the $Cu(OH)_2$ NW film was completely reduced.

Modification of the Cu NW film electrodes is realized by dropping the corresponding modifiers onto the electrode surface. The X-ray photoelectron spectroscopy (XPS) patterns show the successful modification of glycine on the Cu NW film (Figure S2A, see the ESI). Figure 2A shows that bare Cu NW film reveals no signal of nitrogen species while the glycine modified Cu NW film shows a peak at ~400 eV in N1s scan, corresponding to $–NH_2$ group. Such peak is still present on the modified Cu NW film after operating at -1.9 V vs. Ag/AgCl for 6 h, indicating that the modification group is stable during the harsh electrochemical testing. On the bare Cu NW film, there is only one weak peak at ~283 eV in C1s scan, attributing to the sp^2 C–C of trace graphite contaminant. In contrast, there are obvious peaks at ~284, ~286 and ~289 eV in the spectrum of the operated glycine modified Cu NW film electrode, indicating the existence of sp^3 C–C, C–O and –COOH, respectively (Figure S2B, see the ESI). Besides that, peaks at ~532 and ~533 eV in O1s scan for the used glycine modified Cu NW film also suggest the existence of organic O species, while there is only one small metal oxide peak at ~530 eV for the bare Cu NW film (Figure S2C, see the ESI). The presence of all these signals indicates the existence of –COOH and $–NH_2$ functional groups on the modified Cu NW film and further confirms that the adsorption of glycine is stable (Figure S2, see the ESI). Fourier transform infrared spectroscopy (FT-IR) and attenuated total reflection infrared spectroscopy (ATR-IR) patterns in Figure 2B also confirm the successful modification on copper surface. Peaks observed at ~3000 cm^{-1} are ascribed to the stretching vibration of N-H and vibration of associated –COOH. In Figure 2C, the electro-

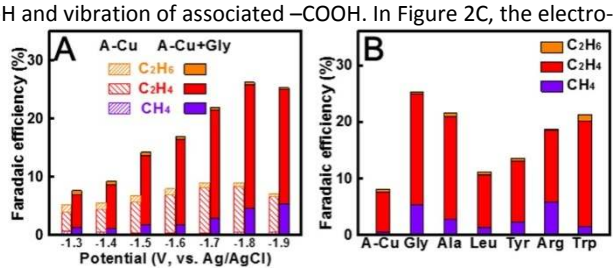

Figure 5. Electrochemical CO_2 reduction on annealed Cu electrodes. (A) On full potential range from -1.3 V to -1.9 V. (B) With different amount of glycine at -1.9 V.

chemical impedance spectroscopy (EIS) also proves the absorption of amino acids on the Cu NW film. After modification with glycine, an obvious semicircle impedance loop appears in the high-frequency region. As the radius of semicircle is related to the charge transfer resistance at the interface of electrode and electrolyte, thus the increase of semicircle diameter (charge transfer resistance) indicates that a stable glycine layer is successful absorbed onto the surface of the Cu NW film by occupying some surface sites. Furthermore, contact angle measurements of the modified Cu NW film in Figure 2D also indicates that the electrode surface is modified, but still maintain its hydrophilicity after the modification (Figure S3, see the ESI). In contrast to the hydrophobic Cu foil surface (109.14°), porous Cu NW film exhibits a hydrophilic surface property (31.3°). The hydrophilic nature of Cu NW film is very important for producing uniformly modified Cu NW films. After modification with 40 µL, 1.0 mM glycine solution, contact angle increases slightly (55.78°). However, the surface remains hydrophilic. This is advantageous for electro-reduction of CO_2 as it ensures sufficient contact area between the electrode and the electrolyte. Modification with large amount of glycine results in a hydrophobic Cu NW film surface (contact angle of 116.26°) which would block the transfer of dissolved CO_2 during electrolysis.

The FEs of various products obtained on Cu NW film with and without the modification of glycine are shown in Figure 3A (products analyses are shown in Figure S4-7 and Table S1, see the ESI). C2 products (C_2H_4 and C_2H_6) with high FEs as well as some C3 products (C_3H_6) are observed on the bare Cu NW film electrode, which is quite different from previously reported results on various Cu electrodes (Table S2, See the ESI). The generation of C3 product is rare, which could be related to the thick and porous nanowire layer. After the glycine modification, hydrocarbon generation is further enhanced while hydrogen evolution is suppressed. The FEs of C_2H_4 and C_2H_6 increase with the decrease of the potential while that of C_3H_6 remains unchanged. At -1.9 V, the total FE of hydrocarbons on the Cu NW film modified with glycine reaches 34.1%, which has almost doubled from the bare Cu NW film electrode (17.8%). Furthermore, the FE of H_2 drops at each potential for the modified electrodes, in alignment with the

increasing selectivity towards hydrocarbons (Table S1, see the ESI). Potentials more negative than -1.9 V are not applied in experiment because the absorbed glycine would detach from the surface at such negative potentials. To evaluate the effect of modification degree, the FEs of total hydrocarbons on Cu NW film electrodes at a typical potential of -1.9 V with varying glycine amounts are examined (Figure 3B). The FEs of total hydrocarbons

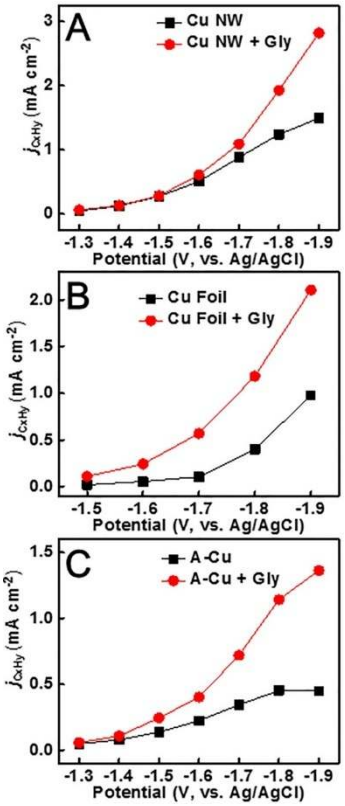

Figure 6. Partial current density of hydrocarbons: (A) Cu NW film electrodes. (B) Cu foil electrodes. (C) Annealed Cu electrodes (A-Cu).

first increased and then decreased with the increase of glycine amount. The FE reaches the maximum of 34.1% at 40 μL×1.0 mM glycine(4×10^{-5} m mol), corresponding to a glycine loading of 4.55×10^{-8} m mol cm^{-2} on Cu NW film (based on electrochemical active surface area). The electrochemical active surface area of Cu NW film increased 110 fold compared with the Cu foil, as verified by the measured capacitance difference (1.25 mF cm^{-2} vs 1.15×10^{-2} mF cm^{-2}, Figure S8, see the ESI). At such a loading, it is estimated to be only 7.6% of Cu NW film is covered by glycine, assuming 1 amino acid (glycine) molecule occupies 6 Cu atoms.[52] The increased FE of hydrocarbons over that on the bare Cu NW film suggests that the enhanced catalytic effect is driven by an appropriate level of surface modification by glycine on Cu surface. With too high surface coverage, it may block large number of active catalytic sites and lead to the inhibition of CO_2 electro-reduction.

To find out whether other amino acid will also function in a similar way, various amino acids including DL-alanine, DL-leucine, DL-tyrosine, DL-arginine and DL-tryptophan are also investigated, with same concentration of 1.0 mM. As shown in Figure 3C, Cu NW film electrodes modified with all kinds of amino acids perform better in producing hydrocarbons compared to the bare Cu NW film electrode. Glycine, the simplest amino acid that only contains –COOH and –NH_2 functional groups, provides a relatively higher hydrocarbons FE of 34.1%. DL-alanine just has an extra methyl group compared to glycine, and gets a lower hydrocarbons FE of 24.3%. Other amino acids with larger branch like DL-leucine, DL-tyrosine, DL-arginine and DL-tryptophan also demonstrate enhanced FEs of hydrocarbons at 19.4%, 20.9%, 23.6% and 27.1%, respectively. The results suggest that –COOH and –NH_2 are probably responsible for the enhanced selectivity of CO_2 reduction. Previous reports illustrate that the adsorption of amino acids on Cu surface is achieved through both –COOH and –NH_2 groups.[52] Stearic acid ($C_{17}H_{35}COOH$, RCO_2H), which contains only –COOH group, is selected to identify the role of –COOH. As shown in Figure 3D, the production of hydrocarbons is weakened when the electrode is modified with stearic acid. Other modifiers such as α-anthraquinone diazonium salt (AQ),[53] o-nitrobenzene diazonium salt ($PhNO_2$),[53] dodecyl mercaptane ($C_{12}H_{25}SH$, RSH) which contain neither –COOH nor –NH_2 groups are also investigated, and all these modifiers reduce the amount of hydrocarbons produced. In particular, the AQ-modified Cu NW film electrodes exhibited only 8.7% of total hydrocarbon FE. The negative effects of other modifiers suggest that amino acids are critical for the electrocatalytic reduction of CO_2 to hydrocarbons. It is proposed that amino acids adsorbed on the catalyst surface which introduce the –NH_2 group can simultaneously enhance hydrocarbon generation.

As the types of Cu electrodes would affect the selectivity of final products of the CO_2 electroreduction, the modification method is extended to other Cu electrodes in order to further demonstrate the validity of this novel modification approach and to rule out the Cu morphology effect on the CO_2 reduction (Figure S9A, see the ESI). Figure 4A shows FEs of CH_4 and C_2H_4 of bare and glycine modified Cu foil electrodes from -1.5 V to -1.9 V. Our Cu foil benchmarks well with the previous report.[54] After modification, the FEs of CH_4 and C_2H_4 of glycine modified Cu foil are clearly higher than those of the bare one at full potential range. The FEs of CH_4 and C_2H_4 achieve 32.1% and 24.0% on the modified Cu foil electrode respectively, while the corresponding FEs of the bare Cu foil electrode are only 16.1% and 9.5%. Similar to the Cu NW electrodes, the largest enhancement of total hydrocarbons FE (30.5%) is also achieved at -1.9 V. Figure 4B exhibits an optimized amount 5×10^{-7} mmol of glycine for the Cu foil electrode (20 mm×20 mm). The corresponding covering rate is estimated to be 10.4%, which is close to that of the modified Cu NW film. In Figure 4C, all kinds of amino acids demonstrate the positive effect in producing hydrocarbons at all tested potentials, while glycine is the best among them (Figure S10, see the ESI). The investigation of other modifiers containing neither –COOH nor –NH_2 groups in Figure 4D further confirms the critical role of amino acid on the promotion of CO_2 conversion efficiency to hydrocarbons.

Furthermore, another kind of Cu electrodes derived from oxides with high activity in producing hydrocarbons is also investigated (Figure S9B and S11, see the ESI).[43] Figure 5A shows the comparison of FEs for various hydrocarbons on bare annealed Cu electrode and modified counterpart. The FE of total hydrocarbons at -1.5 V vs. Ag/AgCl (~0.85V vs. RHE) on our bare annealed Cu electrode is close to the reported value, offering a

good benchmark point.[43] The FEs of both CH_4 and C_2H_4 on glycine-modified electrode is higher than those of the bare one throughout the overall potential range. The total FE of hydrocarbons reached the highest value of 26.2% and 10.3% with and without glycine at -1.8 V, respectively. However, the largest difference of FE is 17.2% at -1.9 V, as shown in Figure 5A. The results in Figure 5B obtained from the annealed Cu electrodes modified by different amino acids again confirm this effective approach, and glycine is still the optimal choice to improve the selectivity of CO_2 conversion to hydrocarbons.

The current density (*j*), which represents the production rate, is further investigated. After modification, the total current density (j_{total}) during the electrolysis decreases. Previous work reported the nanostructured metal electrocatalysts could suppress the hydrogen evolution while enhancing the CO_2 electroreduction, through the complex interplay between surface structure, electrode mesostructure, and the electrolyte composition.[55] In our case, we hypothesize that the current decrease is mainly due to the coverage of modifiers on catalytic active sites for hydrogen evolution reaction, while having minimal influence on hydrocarbon generation (Figure S12, see the ESI). In contrast to the total current density, partial current densities of hydrocarbons (j_{CxHy}) are even higher than that of the bare electrodes, in spite of the partial coverage of active sites by functional molecules. For Cu NW film, Cu foil and annealed Cu electrodes, both j_{CxHy} and the differences of j_{CxHy} between the modified and bare electrodes increase with the decrease of potential. j_{CxHy} shows over 100% increase at -1.9 V for all three kinds of electrodes, as illustrated in Figure 6. The results indicate that the rise of FEs is due to not only the drop of side reaction current density (like hydrogen evolution current density), but also a clearly enhanced capability in producing hydrocarbons after modification. The enhanced selectivity of hydrocarbons is probably related to the strong interaction between $-NH_2$ groups in amino acids and formyl (CHO). The interaction plays a significant role in stabilization and transform of formyl (CHO), which is the most important intermediate of CO_2 electroreduction towards hydrocarbons. Nørskov proposed that the ligands tethered to the electrode surface would interact with the adsorbed CHO and stabilize it,[42] the energy barrier for the formation of CHO would be reduced and subsequent hydrocarbon formation could be facilitated. A Tafel plot, consisted of potential vs. the log of CO current density, is also extracted from the data in an attempt to get more information about the possible mechanism. At lower current density, a Tafel slope of ~0.13 V dec^{-1} indicates the CO_2 electroreduction is at the 1st order with respect to CO_2, and the rate determining step of the reaction is the first electron transfer to CO2 to form $CO2^{\bullet-}$.[43] Before and after modification of the Cu NW film electrodes, the slopes of linear parts are 0.124 and 0.120 V dec^{-1}, respectively (Figure S13, see the ESI). It indicates the modification process do not change the Tafel slopes of Cu NW electrodes. The constant Tafel slopes reveal that the modification would not decrease the overpotential of CO_2 electroreduction while only increasing the hydrocarbons yield. Furthermore, the measurement of Tafel slopes on Cu foil and annealed Cu electrodes are also carried out (Figure S13, see the ESI). The Tafel slopes of Cu foil and annealed Cu electrodes are 0.122 and 0.119 V dec^{-1}, respectively. After modification process, the Tafel slopes remain unchanged, which are 0.119 V dec^{-1} and 0.125 V dec^{-1}, respectively. All these results are consistent with the previous reported values in similar overpotential range and also indicate the modification process of copper electrode will not change the rate determine step ($CO_2 \rightarrow CO_2^{\bullet-}$) in the CO_2 reduction process.[13, 56]

To further unveil the underlying mechanism, the free energy change of CO_2 and CO protonation on bare and glycine modified Cu surface are calculated (Figure 7). Consistent with previous calculations, the key step of CO_2 electroreduction towards hydrocarbon products is the CO* (* denotes adsorbed species) hydrogenation to CHO* with a free energy change of 0.79 eV.[57, 58]

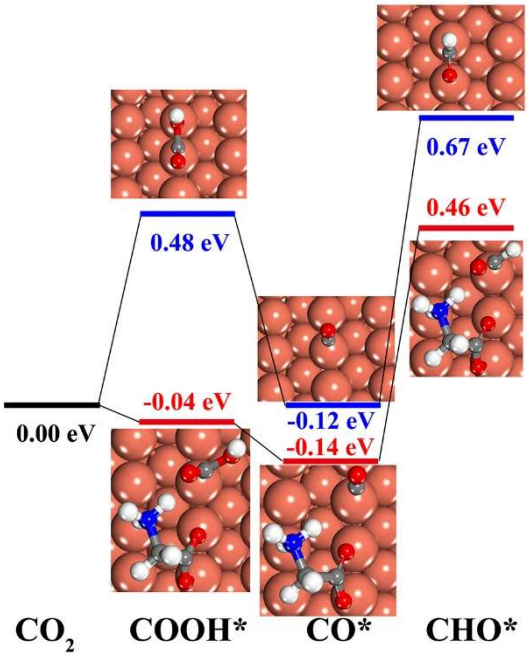

Figure 7. The DFT calculated free energy change of CO_2 and CO protonation without glycine (blue line) and with zwitterionic glycine (red line).

Due to the fact that glycine will partially transfer from neutral to zwitterionic form in the aqueous environment and the experimental pH range, we take into account both glycine forms.[59] In its neutral form, glycine adsorbs on Cu(110) with its $-NH_2$ end while negligible free energy changes are found during CO_2 and CO protonation. However, the $-NH_3^+$ end of zwitterionic glycine exhibits strong hydrogen-bond like interaction with both COOH* and CHO* adsorbate, leading to a stabilization of ~0.50 eV and ~0.20 eV, respectively (Figure S14). Therefore, amino acids adsorbed on the catalyst surface would introduce the $-NH_3^+$ group, stabilize CHO* and simultaneously enhance hydrocarbon generation.

The stability of glycine modified as well as bare Cu NW film electrodes is also evaluated in the electrochemical operation (Figure S15, see the ESI). FE of hydrocarbons remains largely stable for at least 6 h electrochemical reduction of CO_2, and keeps more than 2/3 after 12 h operation. The hydrocarbons FE of glycine modified Cu NW film at 12 h (22.6%) is still obviously larger than that of bare Cu NW film electrode at 1 h (16.7%). Moreover, current density has also remained roughly unchanged at ~11 mA cm^{-2} for the modified Cu NW film electrode and at ~14 mA cm^{-2} for the bare

Cu NW film electrodes during such a long electrochemical operation period. The similar trend of FE and current density changing demonstrates that the modification would be stable. The stable adsorption of amino acids on Cu NW film electrodes during electrolysis is further supported by the XPS results (Figure 8A). The retained Cu NW morphology and similar EIS results further prove the robust structure (Figure S17 and Figure 8B). Both of the robust structure and stable adsorption of amino acids assure the excellent electrochemical stability during the CO_2 reduction.

4 Conclusions

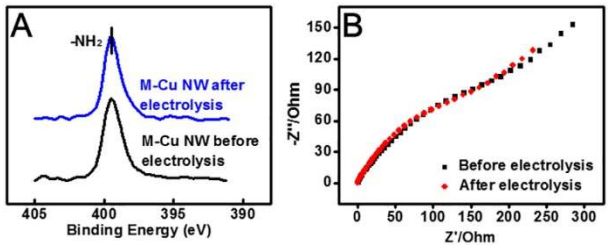

Figure 8. (A) XPS pattern (N1s scan) of the modified Cu NW film, before and after electrolysis at -1.9 V. (B) EIS of the modified Cu NW film, before and after electrolysis at -1.9 V in CO_2 saturated $KHCO_3$ solution.

In summary, we developed a general and effective approach of amino acid modification on Cu electrodes for the enhanced electroreduction of CO_2 towards hydrocarbons. To demonstrate the validity of this novel modification approach and to rule out the possible Cu morphology effect, we examined three different types of Cu electrodes, namely, Cu NW film, polished Cu foil and annealed Cu electrodes. The Cu NW film demonstrated an excellent activity for the generation of C2 and C3 hydrocarbons in the CO_2 electroreduction. Remarkable enhancement in faradaic efficiency as well as partial current density of hydrocarbons is observed for all kinds of Cu electrodes after proper modification. This modification method would suppress hydrogen evolution and improve the efficiency of the total hydrocarbons generated. Theoretical calculations reveal that the hydrogen bond formation between CHO* and $–NH_3^+$ end of zwitterionic glycine leads to an extra stabilization of CHO*, which would contribute to the enhanced selectivity for CO_2 reduction. The results reveal that amino acids and their derivatives are promising modifiers in improving the selectivity of hydrocarbons in CO_2 electroreduction, and this strategy has potential to be extended to other important electrocatalytic reactions.

Author Contributions

M. S. X., B. Y. X. and Y. L. contributed equally to this work. All authors have given approval to the final version of the manuscript.

Conflict of interest

The authors declare no competing financial interests.

Acknowledgment

This project is funded by the National Research Foundation (NRF), Prime Minister's Office, Singapore under its Campus for Research Excellence and Technological Enterprise (CREATE) programme. We also acknowledge financial support from the academic research fund AcRF tier 1 (M4011253 RG 7/14) and tier 2 (M4020246, ARC10/15), Ministry of Education, Singapore.

References

1 K. J. Van Groenigen, C. W. Osenberg and B. A. Hungate, *Nature*, 2011, **475**, 214-216.
2 F. Studt, I. Sharafutdinov, F. Abild-Pedersen, C. F. Elkjær, J. S. Hummelshøj, S. Dahl, I. Chorkendorff and J. K. Nørskov, *Nat. Chem.*, 2014, **6**, 320-324.
3 G. Melaet, W. T. Ralston, C.-S. Li, S. Alayoglu, K. An, N. Musselwhite, B. Kalkan and G. A. Somorjai, *J. Am. Chem. Soc.*, 2014, **136**, 2260-2263.
4 J. Yu, J. Low, W. Xiao, P. Zhou and M. Jaroniec, *J. Am. Chem. Soc.*, 2014, **136**, 8839-8842.
5 Y. Zheng, J. Liu, J. Liang, M. Jaroniec and S. Z. Qiao, *Energy Environ. Sci.*, 2012, **5**, 6717-6731.
6 T. Y. Ma and S. Z. Qiao, *ACS Catal.*, 2014, **4**, 3847-3855.
7 N. P. Wickramaratne, J. Xu, M. Wang, L. Zhu, L. Dai and M. Jaroniec, *Chem. Mater.*, 2014, **26**, 2820-2828.
8 Y. Hori, K. Kikuchi and S. Suzuki, *Chem. Lett.*, 1985, DOI: 10.1246/cl.1985.1695, 1695-1698.
9 M. Gattrell, N. Gupta and A. Co, *J. Electroanal. Chem.*, 2006, **594**, 1-19.
10 J. Qiao, Y. Liu, F. Hong and J. Zhang, *Chem. Soc. Rev.*, 2014, **43**, 631-675.
11 K. Nakata, T. Ozaki, C. Terashima, A. Fujishima and Y. Einaga, *Angew. Chem. Int. Edit.*, 2014, **53**, 871-874.
12 R. J. Lim, M. Xie, M. A. Sk, J.-M. Lee, A. Fisher, X. Wang and K. H. Lim, *Catal. Today*, 2014, **233**, 169-180.
13 Y. Chen, C. W. Li and M. W. Kanan, *J. Am. Chem. Soc.*, 2012, **134**, 19969-19972.
14 S. Zhang, P. Kang and T. J. Meyer, *J. Am. Chem. Soc.*, 2014, **136**, 1734-1737.
15 A. J. Morris, R. T. McGibbon and A. B. Bocarsly, *ChemSusChem*, 2011, **4**, 191-196.
16 C. L. Anfuso, R. C. Snoeberger, A. M. Ricks, W. Liu, D. Xiao, V. S. Batista and T. Lian, *J. Am. Chem. Soc.*, 2011, **133**, 6922-6925.
17 J. A. Keith and E. A. Carter, *J. Am. Chem. Soc.*, 2012, **134**, 7580-7583.
18 C. Costentin, S. Drouet, M. Robert and J.-M. Savéant, *Science*, 2012, **338**, 90-94.
19 B. Kumar, M. Asadi, D. Pisasale, S. Sinha-Ray, B. A. Rosen, R. Haasch, J. Abiade, A. L. Yarin and A. Salehi-Khojin, *Nat. Commun.*, 2013, **4**, 2819-2827.
20 W. Zhu, R. Michalsky, Ö. Metin, H. Lv, S. Guo, C. J. Wright, X. Sun, A. A. Peterson and S. Sun, *J. Am. Chem. Soc.*, 2013, **135**, 16833-16836.
21 J. A. Keith and E. A. Carter, *Chem. Sci.*, 2013, **4**, 1490-1496.
22 Y. Yan, E. L. Zeitler, J. Gu, Y. Hu and A. B. Bocarsly, *J. Am. Chem. Soc.*, 2013, **135**, 14020-14023.
23 M. Z. Ertem, S. J. Konezny, C. M. Araujo and V. S. Batista, *J. Phys. Chem. Lett.*, 2013, **4**, 745-748.
24 H. Mistry, R. Reske, Z. Zeng, Z.-J. Zhao, J. Greeley, P. Strasser and B. R. Cuenya, *J. Am. Chem. Soc.*, 2014, **136**, 16473-16476.
25 A. S. Varela, N. Ranjbar Sahraie, J. Steinberg, W. Ju, H.-S. Oh and P. Strasser, *Angew. Chem. Int. Edit.*, 2015, **54**, 10758-10762.

26 Y. Hori, I. Takahashi, O. Koga and N. Hoshi, *J. Mol. Catal. A-Chem.*, 2003, **199**, 39-47.
27 K. P. Kuhl, E. R. Cave, D. N. Abram and T. F. Jaramillo, *Energy Environ. Sci.*, 2012, **5**, 7050-7059.
28 J. Christophe, T. Doneux and C. Buess-Herman, *Electrocatal.*, 2012, **3**, 139-146.
29 W. Tang, A. A. Peterson, A. S. Varela, Z. P. Jovanov, L. Bech, W. J. Durand, S. Dahl, J. K. Norskov and I. Chorkendorff, *Phys. Chem. Chem. Phys.*, 2012, **14**, 76-81.
30 M. R. Gonçalves, A. Gomes, J. Condeço, T. R. C. Fernandes, T. Pardal, C. A. C. Sequeira and J. B. Branco, *Electrochim. Acta*, 2013, **102**, 388-392.
31 C. W. Li, J. Ciston and M. W. Kanan, *Nature*, 2014, **508**, 504-507.
32 R. Kas, R. Kortlever, A. Milbrat, M. T. M. Koper, G. Mul and J. Baltrusaitis, *Phys. Chem. Chem. Phys.*, 2014, **16**, 12194-12201.
33 R. Kas, R. Kortlever, H. Yılmaz, M. T. M. Koper and G. Mul, *ChemElectroChem*, 2015, **2**, 354-358.
34 S. Rasul, D. H. Anjum, A. Jedidi, Y. Minenkov, L. Cavallo and K. Takanabe, *Angew. Chem. Int. Edit.*, 2015, **54**, 2146-2150.
35 A. S. Varela, C. Schlaup, Z. P. Jovanov, P. Malacrida, S. Horch, I. E. L. Stephens and I. Chorkendorff, *J. Phys. Chem. C*, 2013, **117**, 20500-20508.
36 O. A. Baturina, Q. Lu, M. A. Padilla, L. Xin, W. Li, A. Serov, K. Artyushkova, P. Atanassov, F. Xu, A. Epshteyn, T. Brintlinger, M. Schuette and G. E. Collins, *ACS Catal.*, 2014, **4**, 3682-3695.
37 R. Reske, H. Mistry, F. Behafarid, B. Roldan Cuenya and P. Strasser, *J. Am. Chem. Soc.*, 2014, **136**, 6978-6986.
38 K. P. Kuhl, T. Hatsukade, E. R. Cave, D. N. Abram, J. Kibsgaard and T. F. Jaramillo, *J. Am. Chem. Soc.*, 2014, **136**, 14107-14113.
39 S. Sen, D. Liu and G. T. R. Palmore, *ACS Catal.*, 2014, **4**, 3091-3095.
40 J. H. Montoya, A. A. Peterson and J. K. Nørskov, *ChemCatChem*, 2013, **5**, 737-742.
41 F. Calle-Vallejo and M. T. M. Koper, *Angew. Chem. Int. Edit.*, 2013, **52**, 7282-7285.
42 A. A. Peterson and J. K. Nørskov, *J. Phys. Chem. Lett.*, 2012, **3**, 251-258.
43 C. W. Li and M. W. Kanan, *J. Am. Chem. Soc.*, 2012, **134**, 7231-7234.
44 G. Szollosi, C. Somlai, P. T. Szabo and M. Bartok, *J. Mol. Catal. A-Chem.*, 2001, **170**, 165-173.
45 W. Chen, Y. Y. Zhang, L. B. Zhu, J. B. Lan, R. G. Xie and J. S. You, *J. Am. Chem. Soc.*, 2007, **129**, 13879-13886.
46 G. Kresse and J. Furthmüller, *Phys. Rev. B*, 1996, **54**, 11169-11186.
47 J. P. Perdew, K. Burke and M. Ernzerhof, *Phys. Rev. Lett.*, 1996, **77**, 3865-3868.
48 P. E. Blöchl, *Phys. Rev. B*, 1994, **50**, 17953-17979.
49 Y. Hori, I. Takahashi, O. Koga and N. Hoshi, *Journal of Molecular Catalysis A: Chemical*, 2003, **199**, 39-47.
50 H. J. Monkhorst and J. D. Pack, *Phys. Rev. B*, 1976, **13**, 5188-5192.
51 J. K. Nørskov, J. Rossmeisl, A. Logadottir, L. Lindqvist, J. R. Kitchin, T. Bligaard and H. Jónsson, *J. Phys. Chem. B*, 2004, **108**, 17886-17892.
52 N. A. Booth, D. P. Woodruff, O. Schaff, T. Giessel, R. Lindsay, P. Baumgartel and A. M. Bradshaw, *Surf. Sci.*, 1998, **397**, 258-269.
53 M. C. Bernard, A. Chausse, E. Cabet-Deliry, M. M. Chehimi, J. Pinson, F. Podvorica and C. Vautrin-Ul, *Chem. Mater.*, 2003, **15**, 3450-3462.
54 J. Lee and Y. Tak, *Electrochim. Acta*, 2001, **46**, 3015-3022.
55 A. S. Hall, Y. Yoon, A. Wuttig and Y. Surendranath, *J. Am. Chem. Soc.*, 2015, **137**, 14834-14837.
56 Y. Hori, in *Modern Aspects of Electrochemistry*, eds. C. Vayenas, R. White and M. Gamboa-Aldeco, Springer New York, 2008, vol. 42, ch. 3, pp. 89-189.
57 A. A. Peterson, F. Abild-Pedersen, F. Studt, J. Rossmeisl and J. K. Norskov, *Energy Environ. Sci.*, 2010, **3**, 1311-1315.
58 W. J. Durand, A. A. Peterson, F. Studt, F. Abild-Pedersen and J. K. Nørskov, *Surf. Sci.*, 2011, **605**, 1354-1359.
59 R. Bonaccorsi, P. Palla and J. Tomasi, *J. Am. Chem. Soc.*, 1984, **106**, 1945-1950.

Energy & Environmental Science

ARTICLE

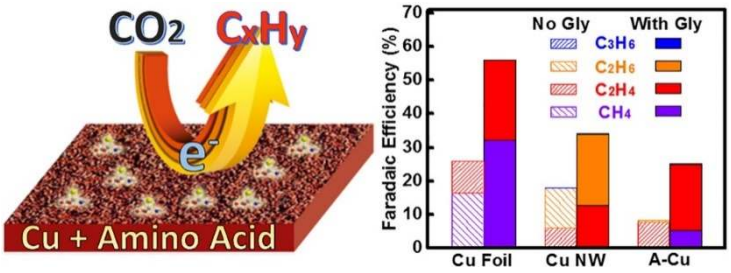

TABLE OF CONTENT

Amino acid functionalized Cu nanowire (NW) film electrode exhibits remarkable enhanced selectivity in producing hydrocarbons. The key intermediate to hydrocarbons, such as CHO, would be stabilized by interacting with amino acid and thus promote the conversion efficiency. This strategy could also be applied to other Cu electrodes to obtain better efficiency towards the conversion of carbon dioxide.